

# Segmental relaxation of water-aged ambient cured epoxy

Guijun Xian, Vistasp M. Karbhari\*

Materials Science and Engineering Program and Department of Structural Engineering, University of California San Diego (UCSD),  
MC-0085, La Jolla, CA 92093-0085, USA

Received 4 February 2007; received in revised form 27 June 2007; accepted 27 June 2007  
Available online 20 July 2007

## Abstract

The effects of long-term immersion on the viscoelastic characteristics of an ambient-temperature cured epoxy system, typical of systems used in infrastructure rehabilitation, are investigated using dynamic mechanical thermal analysis (DMTA). The study considers specimens aged at temperatures of immersion of 23, 37.8 and 60 °C. Time–temperature superposition principles were used to construct master curves of the storage modulus in the glass–rubber transition region for both wet and rejuvenated specimens. Viscoelastic parameters such as the relaxation time and the distribution parameters ( $\beta$ ) were determined using KWW curve fits to the master curves. The free-volume content determined through curve fitting of the WLF is higher by about 0.4% for wet specimens than the rejuvenated specimens. Consequently, the fragility index and the activation energy of the relaxation around  $T_g$  are all reduced in the wet state. The viscoelastic properties of the aged epoxy specimens are strongly dependent on the temperatures of immersion although the level of water uptake in all cases is similar. Formation of multi-bound water molecules leads to the broadest glass–rubber relaxation in the wet state for specimens aged at 37.8 °C in deionized water, whereas the 60 °C aged specimens show the broadest relaxation in the rejuvenated state due to the formation of a heterogeneous network structure.  
© 2007 Elsevier Ltd. All rights reserved.

**Keywords:** Epoxy composites; Water uptake; Relaxation; Cooperativity; Fragility; Glass transition temperature

## 1. Introduction

Epoxy resins, previously widely used in automotive and aerospace applications, are being increasingly used in the rehabilitation of civil infrastructure systems. In these cases the resins, and their ensuing fiber-reinforced composites, are often field cured under ambient conditions, resulting in cases of cure retardation and under-cure, and are expected to provide long service lives exposed to harsh and varying climatic conditions including wide ranges of temperature, humidity, and immersion [1]. Since moisture uptake is known to influence the long-term characteristics of these materials [1–10], its effects under hygrothermal conditions of exposure on the long-term response are of significant interest.

Water molecules are generally held to exist in an epoxy in both the free and the bound states [8,11–13] although there

are some discrepancies reported in the literature based on the experimental results [5,13–15]. Most commonly the sorbed water acts as a plasticizer causing a depression in the glass transition temperature ( $T_g$ ) through interruption of inter-chain hydrogen bonds by the water molecules [4,8] or through the polymer–diluent solution effect [5]. Hahn studied swelling in a polymer composite due to water ingress and reported that although the water initially produces very little swelling, volume is seen to increase proportionally to moisture uptake once a critical absorption threshold is exceeded [16]. Long-term moisture ingress has also been reported to cause irreversible changes leading to degradation of molecular structure [17], formation of microcracks [18], and interfacial debonding in the case of composites [6,19].

Dynamic mechanical thermal analysis (DMTA) has been shown to be a useful tool to investigate the effect of moisture ingress on the viscoelastic response of polymers and polymer composites [6,10,20–23], and characteristics of the loss tangent ( $\tan \delta$ ) curve provide important information related to

\* Corresponding author. Tel.: +1 858 534 6470; fax: +1 858 534 6373.  
E-mail address: [vkarbhari@ucsd.edu](mailto:vkarbhari@ucsd.edu) (V.M. Karbhari).

deterioration and chain mobility. Nogueira et al. suggested that water uptake in the free volume of the polymer structure hinders chain mobility, resulting in a reduction in the height of the peak in the  $\tan \delta$  curve, while water molecules which rupture the interchain hydrogen bonds produce an increment of chain mobility resulting in a reduction in the effective local cross-link density and an increment in the height of the  $\tan \delta$  values [2]. The tightly bound water is noted to cause an increase in the  $T_g$ , which can be identified through drying of the sample which results in a corresponding decrease in  $T_g$  following the removal of residual water content [10]. LaPlante and Lee-Sullivan studied the stress relaxation behavior of an epoxy adhesive and observed that partial saturation of the epoxy resulted in plasticization whereas full saturation resulted in increasing rigidity [24].

DMTA has also been used successfully to study the characteristics of segmental relaxation of cross-linked networks such as relaxation breadth and fragility. The relaxation breadth reflects the range of local environments experienced by the relaxing segments and the corresponding proximity to cross-link junctions [25]. An increase in intermolecular cooperativity is typically encountered at higher levels of cross-linking, with greater sensitivity to time–temperature relations and correspondingly large apparent activation energies being associated with relaxation, which has been linked to increases in the “fragility” of networks with increased cross-linking [26–28]. The viscoelastic characteristics of ambient-temperature cured cross-linked polymers subjected to long-term immersion in water have been shown to depend on the relative dominance of concurrently occurring reversible and irreversible changes in the network, including from post-cure and leaching of low molecular weight flexibilizing species [10].

In the present study the influences of long-term immersion of a typical ambient-temperature cured epoxy, used in infrastructure rehabilitation, on relaxation characteristics and the interaction of sorbed water with the polymer network are investigated as part of a study in predicting long-term durability.

## 2. Materials and experimental methods

The resin system consisted of a 4,4'-isopropylidenephenol-epichlorohydrin (similar to a DGEBA Epon 828 type system) combined with an aliphatic amine hardener (consisting of 10% 4,4'-isopropylidenephenol-epichlorohydrin polymer, 4% tris(2,4,6-dimethylaminomethyl) phenol, 62% blended amines (similar in form to an Epikure 3000 series curing agent) and 24% poly(oxymethyl-1,2-ethanediyl)- $\alpha$ -(2-aminomethylethyl)- $\omega$ -(2-aminomethyl ethoxy)) in a 2:1 ratio, having a gel time of about 60 min at 23 °C. The system was supplied by SCCI under the trade name SCCI Fiber-Matrix I and was specially formulated for SCCI by E-Bond Epoxies, Inc.

Flat panels of 5 mm thickness were cast under ambient-temperature conditions and were allowed to cure at 20–23 °C for 30 days prior to conditioning. It is noted that the cured resin has a density of 1.22 g/cc.

Specimens of size 25 mm  $\times$  25 mm  $\times$  5 mm were cut from the resin plaques using a diamond saw and were immersed in

deionized water at 23, 37.8 and 60 °C in controlled temperature water baths. A set of specimens were also stored in controlled conditions of 23 °C and 30% RH as a reference control. Specimens were removed from the baths at periodic intervals, patted dry with tissue paper and then weighed to measure moisture uptake after which they were reinserted into the baths. At the end of a period of two years specimens were seen to approach an equilibrium level of uptake of about 4% [10]. Aged specimens were carefully cut to thicknesses of 0.5 and 2 mm using a microtome, and all such samples were returned to the corresponding environments for a period of two weeks to equilibrate prior to being tested. In order to rejuvenate, specimens were first dried in vacuum for eight weeks at 60 °C and then the vacuum-dried polymer samples were heated at 150 °C for periods of one and a half hours and then cooled to ambient conditions slowly. Mass loss from drying under vacuum was greater than the 4% equilibrium uptake measured. The increased value was earlier related to a portion of the tightly bond water molecules being removable only at higher drying temperatures [10]. It is also noted that the two-year aged specimens were seen to have reached full cure in about 12 months [10] and hence the rejuvenation treatment is not expected to result in further post-cure, which was validated by the lack of exothermic valleys in the DSC heating profiles resulting from tests on the wet and dried specimens.

A Rheometric Scientific dynamic mechanical thermal analyzer was used to characterize the samples using both single frequency (at 1 Hz) and multi-frequency sweeps (at 0.3, 1, 3, 10 and 30 Hz). Single frequency tests were conducted on specimens of size 10 mm  $\times$  5 mm  $\times$  0.5 mm at a heating rate of 5 °C/min, whereas the multi-frequency tests were conducted on specimens of size 10 mm  $\times$  5 mm  $\times$  2 mm at a heating rate of 2 °C/min. In order to prevent sorbed water from evaporating during the heating ramp the specimens were coated with a very thin film of high temperature vacuum grease and then covered by a 0.13 mm thick polyethylene film (as shown schematically in Fig. 1). The polyethylene film was carefully pressed in order to maintain a uniform thickness of the grease on specimen faces. Preliminary DMTA tests confirmed that the dual configuration (grease and polyethylene) effectively prevented the occurrence of the “drying” effect during testing in the present study, with a well defined peak signifying the minimization of evaporation during testing, which was also validated by gravimetric measurements. Fig. 2(a) and (b) shows a typical set of loss tangent curves showing the difference in results from the treatment. It



Fig. 1. Schematic of the specimen with coatings in preparation for DMTA.

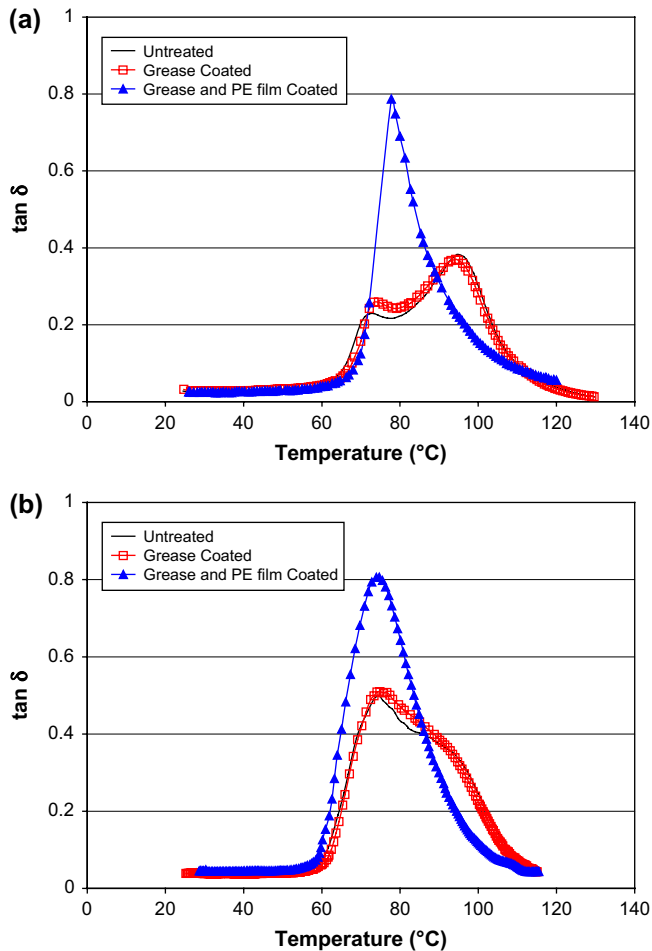


Fig. 2. Typical loss tangent curves showing effect of specimen preparation. (The specific specimen set was aged by immersion in deionized water at 37.8 °C.) (a) Specimen tested in single frequency mode at a heating rate of 5 °C/min. (b) Specimen tested in multiple frequency mode at a heating rate of 2 °C/min.

should be noted that Fig. 2(a) is based on tests conducted at 1 Hz in single frequency mode at a heating rate of 5 °C/min, whereas Fig. 2(b) is at the same frequency but from tests conducted in multi-frequency mode at a heating rate of 2 °C/min. A comparison of the figures shows that, as reported earlier [10], the use of a slower heating rate in untreated samples results in a more pronounced and better defined loss tangent ( $\tan \delta$ ) peak, as well as a change from the splitting mode of the  $\tan \delta$  peak to the formation of only a single peak matching closely in temperature to the lower peak. It can be seen that the grease and PE film treated samples show very close response emphasizing the efficacy of this method of preparation irrespective of heating rate. It is noted that the similarity in response is useful to enable comparison between sets since the fidelity of the curve can potentially be decreased and important features could be obscured by factors such as thermal lag, scanning rate and rates of heating [29,30]. In this case as seen from Fig. 2(a) and (b) the peak height and position are relatively unchanged.

While the initial degree of cure of the system was unfortunately not ascertained, an approximate assessment can be

made following the approach used by Chang et al. [31] to obtain cross-linking density from molecular weight,  $M_c$ , between cross-linking points expressed as a function of the shift of glass transition temperature as:

$$M_c = \frac{39,000}{(T_g - T_{g0})} \quad (1)$$

where  $T_{g0}$  is the glass transition temperature of the uncross-linked polymer. For the current system  $T_{g0}$  is 237 K, and based on measurement of glass transition temperatures there is a decrease in  $M_c$  of about 9% over the unexposed specimens, indicating a corresponding level of increase in polymerization due to post-cure. It is noted that this is essentially achieved in the first 12 months as reported in a previous study on the same system [10]. It is of interest to note that the decreases in  $M_c$  at the end of 24 months of immersion in deionized water at 23, 37.8 and 60 °C were of the order of 7%, 9% and 10%, respectively.

### 3. Results and discussion

#### 3.1. Glass–rubber relaxation

Loss tangent and storage modulus curves for specimens tested immediately after removal from the water baths, at the end of the two-year period of ageing, are shown in Fig. 3(a) and (b) for specimens tested at 1 Hz in single frequency mode at a heating rate of 5 °C/min, and Fig. 3(c) and (d) at the same frequency but from tests conducted in multi-frequency mode at a heating rate of 2 °C/min. The comparison is shown, as in the case of Fig. 2, to indicate that in the current case despite loss of some fidelity at the higher rates of heating the essential characteristics are similar. A summary of dynamic mechanical properties is given in Table 1(a) and (b) for these two test conditions and it can be seen that results pertaining to the loss tangent characteristics are essentially close in both cases. Moduli reported in Table 1 are averages of multiple measurements with standard deviations in all cases being less than 10%. Hygrothermal ageing is seen to result in a decrease in both the glass transition temperature and the loss tangent peak as compared to the unexposed “control” specimen. The well defined loss tangent peaks of the hygrothermally aged specimens clearly indicate the efficacy of the dual grease–polyethylene sealing configuration, and provide further support for the earlier reported hypothesis [10] that the split in the loss tangent peaks in hygrothermally aged specimens is due to drying effects during the DMTA test itself.

The influence of moisture uptake can be clearly seen in Table 1 from the significant difference in the glass transition temperature of the unexposed control specimens (92.1 °C) as compared to the range for specimens immersed in water (69.9–78.3 °C). It is noted that although the level of moisture uptake at all three temperatures was approximately the same, there are clear differences in the dynamic properties. As seen in Fig. 3(a) and (c) immersion in deionized water at 23 °C causes the largest drop in  $T_g$  whereas the least drop is in

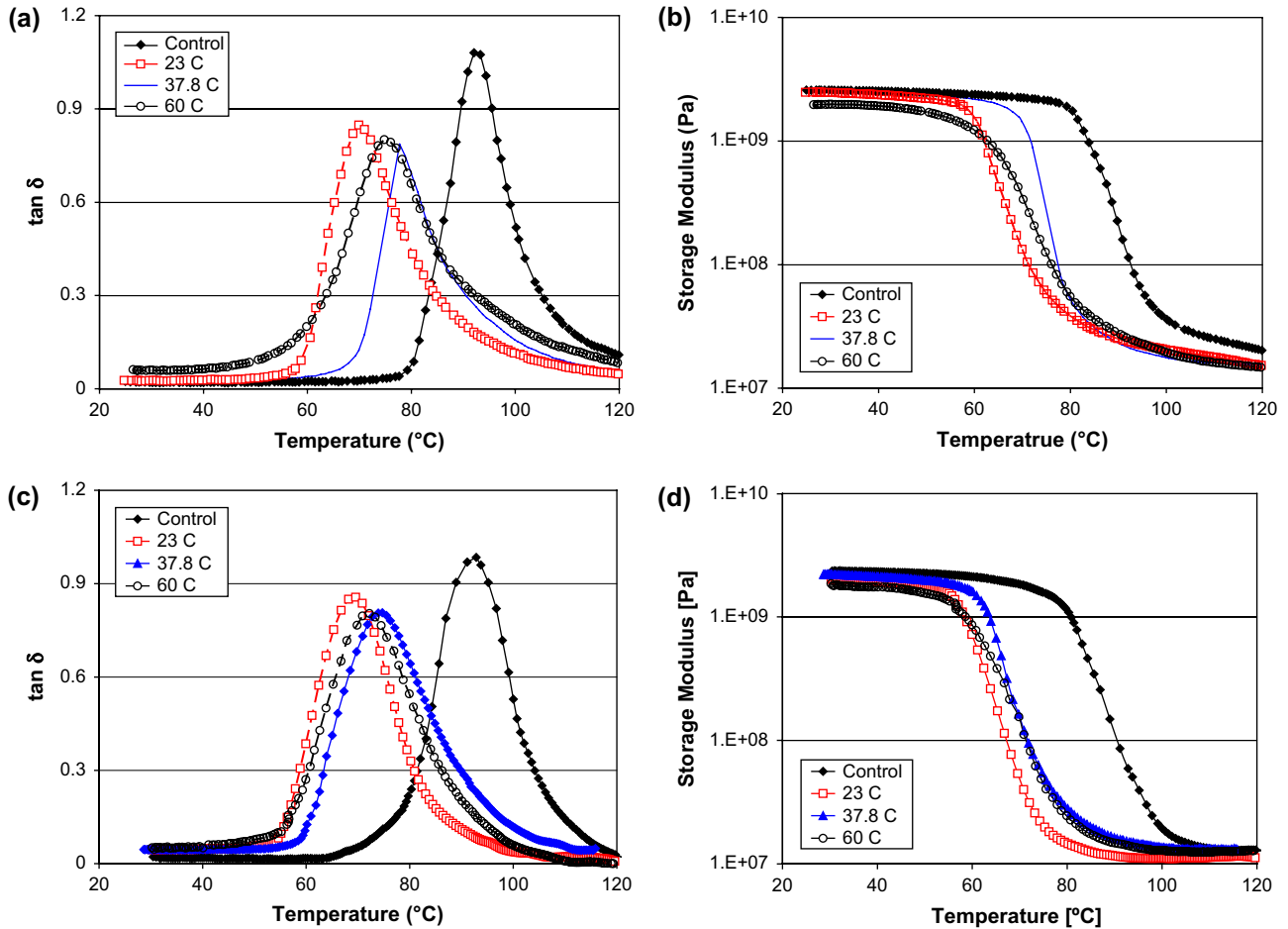


Fig. 3. Effect of immersion in deionized water for 24 months on: (a) loss tangent curves and (b) storage modulus (DMTA test conditions: 5 °C/min from 25 to 120 °C at 1 Hz with a preload strain of 0.01%); (c) loss tangent curves and (d) storage modulus (DMTA test conditions: 2 °C/min from 25 to 120 °C at 1 Hz with a preload strain of 0.01%).

specimens immersed in deionized water at 37.8 °C. The variation in level with immersion temperature can be attributed to the competing effects of residual post-cure [10], interactions between the absorbed water molecules and polar groups in the epoxy [8], the swelling of parts of the polymer structure

[4,32], hydrolysis and chain scission at higher temperatures [7], and microcracking. These effects are also seen through changes in the height of the loss tangent peak and the values of the storage moduli. It is noted that specimens immersed in deionized water at 60 °C exhibited a clearly visible surface

Table 1(a)  
Characteristics of wet and rejuvenated specimens determined by DMTA test in single frequency mode (1 Hz, at a heating rate of 5 °C/min for 0.5 mm specimens)

	Specimens	$T_g$ [°C]	tan $\delta$ peak height	Storage modulus [MPa]	
				Glassy [GPa]	Rubbery [MPa]
Wet	Control	92	1.08	2.6	15.0 <sup>a</sup>
	23 °C water aged	70	0.85	2.5	15.3
	37.8 °C water aged	78	0.78	2.5	15.6
	60 °C water aged	75	0.8	2.0	14.8
Rejuvenated	Control	98	1.03	2.6	14.8
	23 °C water aged	92	0.91	2.7	13.0
	37.8 °C water aged	99	1.07	2.6	14.8
	60 °C water aged	101	0.87	2.8	13.7

<sup>a</sup> The rubbery modulus is taken at 140 °C rather than 120 °C, at which the rubbery plateau is not reached for controlled specimens.

Table 1(b)  
Characteristics of wet, and rejuvenated specimens determined by DMTA test in multi-frequency mode (at 1 Hz, at a heating rate of 2 °C/min for 2 mm specimens)

	Specimens	$T_g$ [°C]	tan $\delta$ peak height	Storage modulus [MPa]	
				Glassy [GPa]	Rubbery [MPa]
Wet	Control	93	1.0	2.4	12.9 <sup>a</sup>
	23 °C water aged	70	0.9	2.0	11.0
	37.8 °C water aged	75	0.8	2.2	13.3
	60 °C water aged	72	0.8	1.8	12.5
Rejuvenated	Control	97	1.0	2.2	12.3
	23 °C water aged	91	0.98	2.0	11.6
	37.8 °C water aged	99	0.9	2.1	13.2
	60 °C water aged	100	0.9	2.1	12.3

<sup>a</sup> The rubbery modulus is taken at 140 °C rather than 120 °C, at which the rubbery plateau is not reached for controlled specimens.

discoloration ranging from light yellow to dark brown, which is indicative of hydrolysis and chain scission. In addition microcracks and crazes were also visible on the surface.

The height of the loss tangent peak is related to the degree of mobility of polymer chains at the glass transition, and is used as a measure of energy dissipation. As can be seen from Fig. 3(a) and (c) the height of the loss tangent peak decreases with immersion in water. The level of reduction increases between the 23 and 37.8 °C cases and is approximately constant at the higher temperatures. This decrease in the height of the loss tangent peak cannot be explained on the basis of plasticization. Nogueira et al. suggested that absorbed water molecules occupying the free volume of the polymer hinder chain mobility and thus cause a reduction in height of the peak [2]. This explanation, however, is questionable since the  $T_g$  is seen to decrease rather than increase as would be expected through conventional water uptake [2,10]. Following Pascault et al. [33] a more probable explanation is that the water molecules interrupt the tightly bound interchain hydrogen bonds, leading to an increase in the number of mobile chain segments around the  $T_g$ , especially in regions of highly packed structure. This is often seen at the initial stage of water uptake [21], and results in an increase in the height of the loss tangent peak. On the other hand, the existence of water in the polymeric structure reduces interchain coherence and/or friction, which is believed to reduce the amount of energy dissipated, during dynamic strain, and thus also the extent of  $\tan \delta$ . The occurrence of an initial increase in  $\tan \delta$  followed by a decrease in epoxies immersed in water was earlier reported by Karbhari [21].

Fig. 3(b) and (d) depicts storage modulus curves for the control and water-aged specimens. With the exception of specimens aged in water at the highest temperature, 60 °C, the differences in glassy storage moduli are negligible, which is in line with results reported elsewhere [34,35]. The storage modulus in the glassy state is a complex function of the overall resin density and cannot be directly related to the cross-link density or the moisture content [34,36]. The 60 °C water-aged specimen possesses the lowest glassy modulus, suggesting that the water absorbed by samples at 60 °C has a higher plasticization effect on the glassy modulus, e.g. plasticizing the highly compact network structures. It is of interest to note that all aged specimens show remarkably similar values of rubbery moduli (as in Fig. 3(b) and (d)) indicating very little change in levels of cross-linking [31].

To further elucidate the influence of water ingress on the viscoelastic characteristics of the epoxy system under consideration, DMTA tests were performed on the rejuvenated specimen films, which were dried at 40 °C under vacuum, and then high temperature treated at 150 °C for half an hour. Comparisons of  $\tan \delta$  and storage modulus curves are presented in Fig. 4(a) and (b), respectively, for the specimens tested at a heating rate of 5 °C/min, and in Fig. 4(c) and (d) for specimens tested at a heating rate of 2 °C/min. Viscoelastic response parameters are also summarized in Table 1. Clearly, drying and high temperature treatment (referred to as the rejuvenation/refreshing treatment) improve the  $T_g$ s of all specimens significantly, which is attributed to the removal of the water causing plasticization

during the period of immersion. Specimens immersed in water at the lowest temperature, 23 °C, exhibit the lowest  $T_g$  compared to the others after rejuvenation, which is about 5–8 °C lower than others. This may indicate a lower effect of residual post-cure resulting from immersion at 23 °C. The increment of  $T_g$ s for the higher temperature immersions (37.8 and 60 °C) is attributed to a combination of both post-curing and leaching of lower molecular weight species [21].

With the exception of specimens aged at the highest temperature of deionized water immersion, 60 °C, the glassy moduli of dried and high temperature treated specimens are almost the same as those of the wet specimens. Similarly, there is an insignificant change in the levels of rubbery moduli for all specimens after the rejuvenation treatment despite a higher variation compared to the wet specimens (Table 1). This again indicates that immersion in deionized water at those temperatures does not influence the cross-linkage significantly. However, it should be emphasized that the 60 °C water immersion over a period of two years results in irreversible degradation reflected by surface cracks and surface discoloration, attributed to the onset of irreversible changes in viscoelastic response.

### 3.2. Time–temperature superposition

In this section, the time–temperature superposition method [37] is used to establish the modulus–time (frequency) master curves over the entire range of the glass–rubber relaxation, and to assess the influence of the ageing of specimens in water on viscoelastic properties. The reference temperature was taken as the peak of the loss tangent curve resulting from DMTA tests at 1 Hz, and was adopted to construct the master curves as shown in Fig. 5(a) and (b) for wet specimens and rejuvenated specimens, respectively. Data are plotted in terms of modulus versus  $1/2\pi f\alpha_T$ , where  $f$  is expressed in hertz and  $\alpha_T$  is the dimensionless shift factor.

Glass–rubber relaxation can be described using a modified version of the Kohlrausch–Williams–Watts (KWW) “stretched exponential” relaxation time distribution function [24,38] as:

$$E(\tau) = E_\infty + (E_0 - E_\infty) \exp \left[ - \left( \frac{\tau}{\tau_0} \right)^\beta \right] \quad (2)$$

where  $E$  is the relaxation modulus,  $E_0$  is the instantaneous modulus ( $E$  at  $\tau = 0$ ),  $E_\infty$  is the relaxed or long-term modulus ( $E_\infty$  at  $\tau = \infty$ ),  $\tau$  is the reduced time variable ( $\tau = t/\alpha_T$ ),  $\tau_0$  is the relaxation time at the reference temperature, and  $\beta$  is the distribution parameter.  $\beta$ , which is inversely related to the broadness of the relaxation process, ranges from 0 to 1 [24,39]. The coupling model [40] can be used to relate the degree of broadening to the extent of intermolecular cooperativity, which in turn can be correlated to the polymer chain structures. The relaxation parameters obtained from curve fitting Eq. (2) to the experimental data in Fig. 5 are presented in Table 2. Moduli listed in Table 2 are determined through use of master curves from the KWW equation with  $R^2 > 0.99$ .

As shown in Table 2, the value of  $E_0$  varies slightly between the wet and rejuvenated specimens, indicating the relative



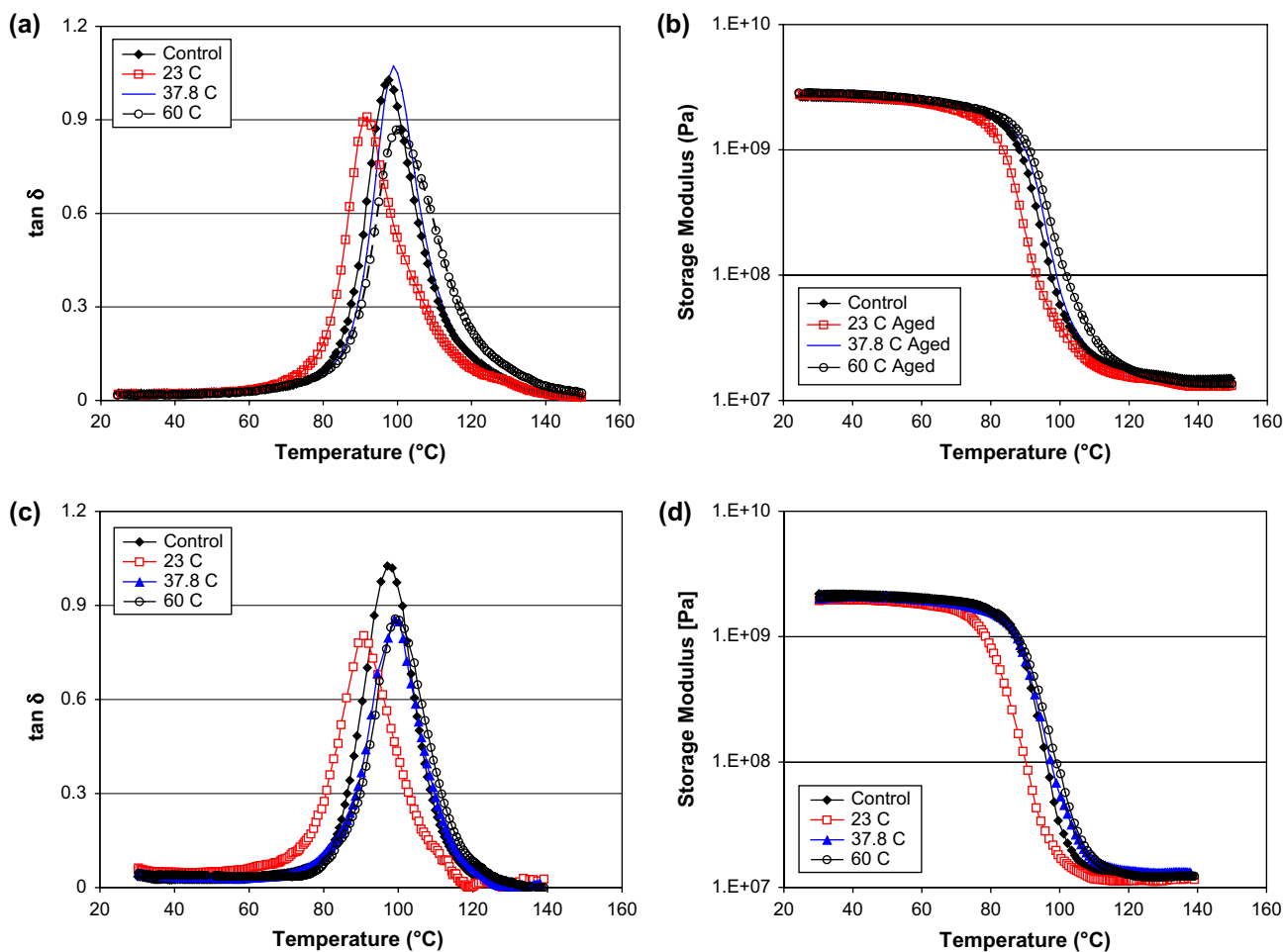


Fig. 4. Effect of rejuvenation of specimens previously aged for 24 months through immersion in deionized water on: (a) loss tangent curves and (b) storage modulus (DMTA test conditions: 5 °C/min from 25 to 150 °C at 1 Hz with a preload strain of 0.01%); (c) loss tangent curves and (d) storage modulus (DMTA test conditions: 2 °C/min from 25 to 150 °C at 1 Hz with a preload strain of 0.01%).

insensitivity of this parameter to water uptake and long-term water ageing, which is in line with results reported by Xian and Karbhari [10] and LaPlante and Lee-Sullivan [24]. Similarly, the values of  $E_{\infty}$  also show very little variation across specimens, suggesting very little change in levels of cross-linking.

For both wet and rejuvenated specimens, ageing conditions are seen to have a significant effect on the values of  $\beta$  (Table 2). For, wet specimens, specimens aged in deionized water at 37.8 °C, possess the lowest  $\beta$  (0.16), and thus exhibit the widest relaxation time distribution. Specimens aged at 23 and 60 °C show a value of  $\beta$  around 0.2, while the unexposed “control” specimens indicate an intermediate value of 0.18.

The relaxation time distribution of the polymer specimens with saturated water ingress is dependent not only on the polymer structures resulting from irreversible aspects such as post-curing, hydrolysis, and leaching, but also on the state of the water molecules. The plasticization effect of the absorbed water causing an increase in free volume or breakage of the strong intermolecular hydrogen bonds [9] is believed to cause a lower extent of cooperativity and thus an increased level in  $\beta$ . However, the distribution of water molecules [4] as well as the presence of multi-bound water molecules [9] which act as cross-linking bonds may broaden the relaxation spectrum and

inversely lead to the decrease of  $\beta$ . Illuminating results regarding details of these interactions were recently reported by Karlsson et al. [41] based on molecular dynamic simulations. On the other hand, post-curing through water immersion at elevated temperatures enhances the extent of cross-linking and increases the intermolecular cooperativity, thus leading to a decrease of  $\beta$  [24,39]. Finally, in the glass–rubber transition region, the activated polymer segments may facilitate the water molecules forming new hydrogen bonds and/or breakage of the formed bonds, and their redistribution in the polymer structure. Such changes are hypothesized to affect the relaxation time distribution and the value of  $\beta$ . Due to the number of potential mechanisms, some acting in opposition to others, it is difficult to accurately determine the cause of the variation of  $\beta$  for the wet specimens. Nevertheless, the lowest  $\beta$  resulting from ageing in deionized water at 37.8 °C can be attributed to the state of the water molecules since the irreversible post-curing effect is not significantly different from the control and 60 °C aged specimens as suggested by the relative similarity in levels of  $T_g$  of the rejuvenated specimens.

Rejuvenated specimens, which have been completely dried can be used to assess the effects of the long-term water immersion. After rejuvenation,  $\beta$  of the specimens immersed in

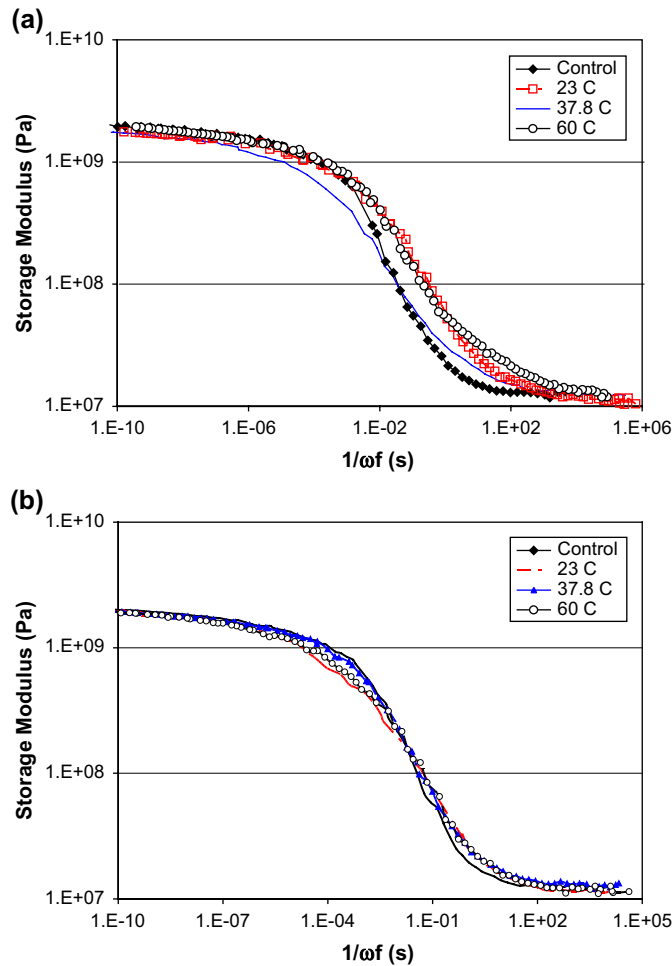


Fig. 5. Time–temperature superposition master curves using  $T_{\text{ref}}$  as the glass transition temperature determined by the peak of the loss tangent curve obtained at 1 Hz: (a) wet specimens and (b) rejuvenated specimens.

37.8 °C deionized water increases from 0.16 in the wet state to 0.19. The initial low value of  $\beta$  for these specimens is primarily due to water ingress. Therefore, it is not surprising that rejuvenation restores the levels. However, the rejuvenation treatment is seen to have an insignificant effect on  $\beta$  of the control and 23 °C water-aged specimens, but causes a decrease in  $\beta$  of the 60 °C aged specimen from 0.21 to 0.16. Immersion in deionized water at the highest level of temperature, 60 °C, is

Table 2

KWW parameters ( $R^2 > 0.99$ ) for the glass–rubber relaxation in the wet and rejuvenated specimens ( $T_{\text{ref}} = T_g$ )

	Specimens	$E_0$ [GPa]	$E_\infty$ [MPa]	Relaxation time [ $10^{-4}$ s]	$\beta_{\text{kww}}$
Wet	Control	2.1	12.5	2.6	0.18
	23 °C water aged	1.9	10.9	2.0	0.2
	37.8 °C water aged	2.1	12.7	1.0	0.16
	60 °C water aged	1.8	12.0	4.7	0.21
Rejuvenated	Control	2.0	12.4	3.0	0.2
	23 °C water aged	2.0	11.5	2.0	0.18
	37.8 °C water aged	2.1	12.3	4.2	0.19
	60 °C water aged	2.1	12.5	1.1	0.16

seen to result in the maximum extent of post-curing (as indicated by the highest value of  $T_g$  of the rejuvenated specimen), and, as expected, more pronounced levels of irreversible reactions (i.e., hydrolysis, leaching, forming microvoids, etc.) are responsible for the greater heterogeneity in the polymer structure and the decreased value of  $\beta$ .

The shift factor above the  $T_g$ , obtained during the construction of the master curves, can be successfully described through use of the WLF equation as:

$$\log \alpha_T = \log \frac{\tau(T)}{\tau(T_{\text{ref}})} = -\frac{C_1(T - T_{\text{ref}})}{C_2 + (T - T_{\text{ref}})} \quad (3)$$

where  $\alpha_T$  is the shift factor at temperature  $T$ ,  $\tau$  is the relaxation time,  $C_1$  and  $C_2$  are parameters dependent on the material and the reference temperature,  $T_{\text{ref}}$ . The fit is shown in Fig. 6, as a solid line with a correlation coefficient,  $R^2$ , of 0.999. Eq. (3) is valid over the temperature ranging from  $T_g$  to  $T_g + 100$  °C. In the present case,  $T_{\text{ref}}$  is selected at  $T_g$  which is determined by the peak of  $\tan \delta$  at 1 Hz. A linear relation can be observed in the temperature range around the  $T_g$ , as previously reported by Adam and Gibbs [27]. Values of the parameters  $C_1$  and  $C_2$  are presented in Table 3. Following Ref. [37], the free volume ( $f$ ) at  $T_g$  and the thermal expansion coefficient ( $\alpha$ ) can be determined using the values of  $C_1$  and  $C_2$  at  $T_g$  as:

$$f = B/2.303C_1 \quad (4)$$

$$\alpha = B/2.303C_1C_2 \quad (5)$$

where  $B$  is the numerical constant and is generally set equal to unity for the sake of simplicity [37]. Values of  $f$  and  $\alpha$  are listed in Table 3.

As shown in Table 3, immersion of specimens in deionized water results in a free-volume content of about 0.4% higher than that in the corresponding rejuvenated specimens. This suggests that the water ingress is associated with an increase in free

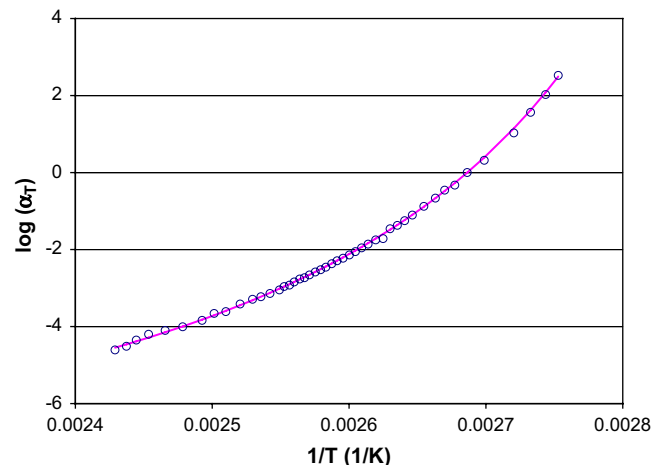


Fig. 6. Typical temperature dependence of the shift factor for a rejuvenated 37.8 °C immersed specimen. The solid line represents curve fit of the WLF equation in the temperature range of  $T_g$  to  $T_g + 40$  °C.

Table 3  
Glass–rubber relaxation characteristics for the wet rejuvenated specimens  
( $T_{\text{ref}} = T_g$ , and  $R^2 > 0.99$ )

Specimens		$C_1$	$C_2$	$f$	$\alpha$	$E_a$	$m$
		[°C]	[°C]	[%]	[ $10^{-4}$ ]	[kJ/mol]	
Wet	Control	11.0	62.7	4.04	7.18	431	68.6
	23 °C water aged	10.7	59.6	4.09	7.01	407	66.9
	37.8 °C water aged	9.5	41.6	4.66	11.9	499	75.1
	60 °C water aged	9.7	44.6	4.49	10.1	443	64.3
Rejuvenated	Control	9.1	41.0	4.75	11.6	550	77.6
	23 °C water aged	11.9	48.6	3.70	7.72	575	82.4
	37.8 °C water aged	10.4	45.5	4.21	9.32	573	80.4
	60 °C water aged	10.7	49.2	4.07	8.27	552	77.4

volume as proposed by Apicella et al. [42]. The higher free-volume content of the wet specimen is believed to be one of the primary reasons for the reduction in the glass transition temperature of specimens. It can also be seen that use of the higher immersion temperatures (37.8 and 60 °C) leads to a higher free volume in the wet samples, which is attributed to more water molecules entering into the compact polymer structures.

Cooperativity, or fragility, plots [ $\log(\alpha_T)$  vs.  $T_g/T$ ] were constructed to further examine the time–temperature superposition characteristics of the glass–rubber relaxation of the wet and rejuvenated specimens. Rizos and Ngai [43] suggested that the implication of the many-body complex aspects of molecular dynamics of relaxation are that the motion of molecular units had to be cooperative in that units needed to move in sequence with some moving before others. As proposed by Adam and Gibbs [27], cooperativity implies that the rearranging movement of a molecule is possible only if a specific number of neighboring molecules are also moved. Polymers with a high level of cooperativity are known to show viscoelastic properties that exhibit stronger temperature dependence of the time–temperature shift factors in the glass transition region [44], which can be quantified in terms of the dynamic fragility of the materials. Fig. 7(a) and (b) (plotted following the commonly used Angell plot format as used previously in Ref. [27]) shows representations of cooperativity plots for the water aged and rejuvenated epoxy specimens, respectively, based on the glass transition temperatures listed in Table 2. It is noted that the slope of the cooperativity curve evaluated at  $T = T_{\text{ref}}$  corresponds to the fragility index,  $m$ , which can be determined as:

$$m = \left. \frac{d \log(\tau)}{d(T_{\text{ref}}/T)} \right|_{T=T_{\text{ref}}} = \left. \frac{d \log(\alpha_T)}{d(T_{\text{ref}}/T)} \right|_{T=T_{\text{ref}}} \quad (6)$$

The value of  $m$  depends on the definition of  $T_{\text{ref}}$ , with the convention being that for the glass transition,  $T_{\text{ref}}$  is assigned such that the corresponding relaxation time  $\tau(T_{\text{ref}}) = 100$  s [26]. The value of  $m$  can also be related to the apparent activation energy ( $E_a$ ) at  $T_{\text{ref}}$  [26,27] as:

$$m = \frac{E_a(T_{\text{ref}})}{2.303RT_{\text{ref}}} \quad (7)$$

where  $R$  is the universal gas constant. For the fragility values reported in this study,  $T_{\text{ref}} = T_g$ . The values of  $m$  and  $E_a$  in Eq.

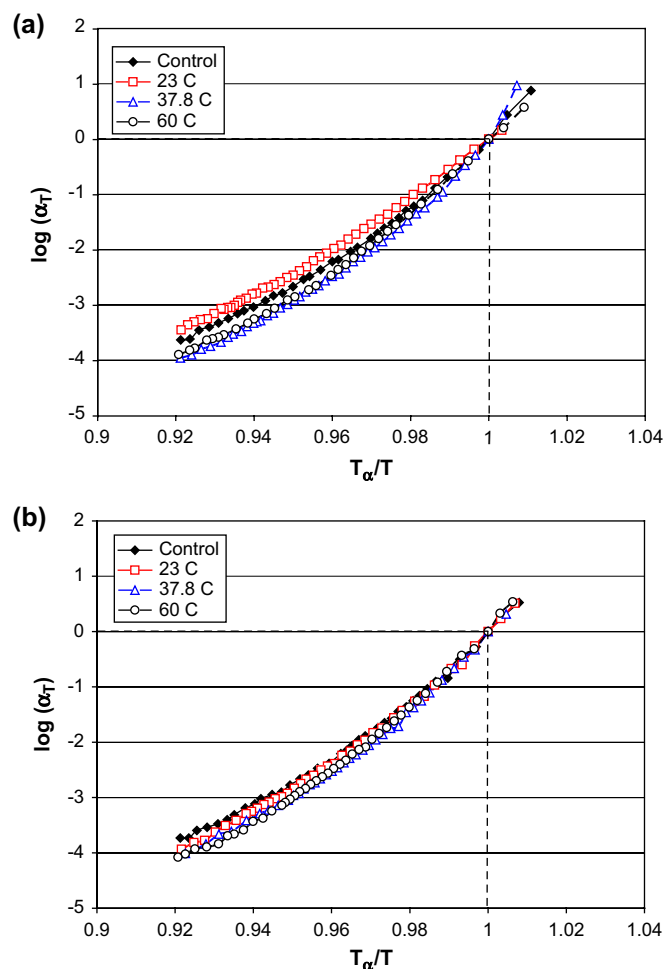


Fig. 7. Cooperativity plots for (a) wet specimens and (b) rejuvenated specimens.

(7) related to Fig. 8 are reported in Table 3, from which it can be seen that the 37.8 °C water-aged specimen have a higher value of the fragility index,  $m = 75.1$ , than the other specimens, indicating a higher degree of intermolecular coupling. This is attributed to the multi-bound water molecules which serve as linkage, as mentioned earlier related to the relaxation distribution,  $\beta$ . As seen from Table 3 the rejuvenated specimens exhibit an evident increase in the fragility index,  $m$ , compared to the wet specimens. Clearly, this is due to the plasticization effect of water ingress, increasing the free-volume content and reducing the intermolecular bonds (e.g., hydrogen bonds), thus decreasing the level of intermolecular coupling.

The activation energy ( $E_a$ ) at  $T_g$  for the shift factor indicates the level of the energy barrier that must be overcome for molecular relaxation. The wet specimens show values of activation energy lower than those of the rejuvenated ones (Table 3). Similar to the case of the variation of fragility index, this clearly reflects the role of water ingress in facilitating polymer relaxation, which is realized through the effects such as the formation of higher free-volume content, the breakup of tight intermolecular hydrogen bonds, and swelling as reported by Adamson [4].



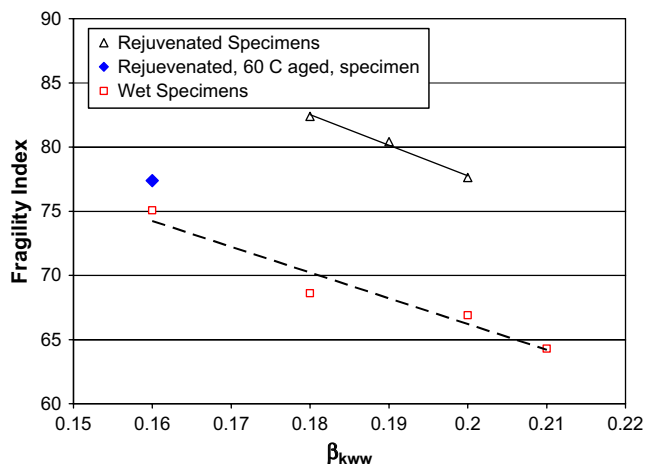


Fig. 8. Fragility index ( $m$ ) as a function of the KWW distribution parameter ( $\beta_{KWW}$ ) for wet and rejuvenated specimens.

The increase of the fragility of the polymer indicates enhanced intermolecular coupling and cooperativity, which contributes to an increase in the distribution of the relaxation times [26,28,44,45]. The correlation is plotted in Fig. 8 for both wet and rejuvenated epoxy structures. Good linear fits ( $R^2 = 0.99$  for the dried specimens and  $R^2 = 0.94$  for the wet specimens) are noted for the specimens except in the case of rejuvenated specimens from 60 °C water ageing. The lower  $\beta$  value of the rejuvenated 60 °C water-aged epoxy is attributed to the high heterogeneity of molecular structure which is reflected by the dark brown skin layer in contrast to the light yellow coloring seen in the core and on other specimens). Compared to the rejuvenated specimens, the wet specimens exhibit a relatively lower value of  $\beta$  with comparative fragility indices as shown in Fig. 8, representative of a broad relaxation time distribution. This is an expected outcome of the complicated water state in the polymer structure and the possible water redistribution, or motion, during the DMTA test.

#### 4. Conclusions

Dynamic mechanical thermal analysis was used to investigate the effects of the long-term water immersion on the viscoelastic properties of an ambient-temperature cured epoxy resin system typical of materials used in rehabilitation of civil infrastructure. The viscoelastic properties of the aged epoxy specimens are shown to be strongly dependent on the immersion temperature, although the level of water uptake is similar under the three temperature conditions used in the study. Water uptake at the lowest temperature of immersion, 23 °C, results in the lowest glass transition temperature,  $T_g$ . Effects of increase in temperature of immersion are seen to be negative on both the rubbery and the glassy moduli after drying, although immersion at the highest temperature, 60 °C, clearly showed degradation in the level of the glassy modulus.

Time–temperature superposition principles were successfully applied to the wet and rejuvenated epoxy structures to construct master curves of the storage modulus in the glass–

rubber transition region. KWW curve fits of the storage master curves indicate a significant dependence of the glass–rubber relaxation for wet and rejuvenated specimens on the temperatures of immersion. The 37.8 °C deionized water-aged specimens exhibited the broadest glass–rubber relaxation in the wet state due to the presence of multi-bound water molecules, whereas the 60 °C aged specimens showed the broadest relaxation in the rejuvenated state due to the resulting heterogeneous polymer structure.

The WLF equation was successfully applied to fit the shift factors above the  $T_g$ , to enable determination of viscoelastic parameters. It was found that water ingress leads to a higher free-volume content of about 0.4% than in the rejuvenated specimens. In addition, water ingress reduces the fragility of the epoxy. In wet conditions, the 37.8 °C water-aged specimens showed the highest  $m$ , corresponding to the lowest  $\beta$ .

#### References

- [1] Abanilla MA, Li Y, Karbhari VM. Durability characterization of wet layup graphite/epoxy composites used in external strengthening. *Composites Part B* 2006;37(2–3):200–12.
- [2] Nogueira P, Ramirez C, Torres A., Abad MJ, Cano J, Lopez J, et al. Effect of water sorption on the structure and mechanical properties of an epoxy resin system. *J Appl Polym Sci* 2001;80(1):71–80.
- [3] Adams RD, Singh MM. The dynamic properties of fibre-reinforced polymers exposed to hot, wet conditions. *Compos Sci Technol* 1996;56(8):977–97.
- [4] Adamson MJ. Thermal-expansion and swelling of cured epoxy-resin used in graphite-epoxy composite-materials. *J Mater Sci* 1980;15(7):1736–45.
- [5] Apicella A, Nicolais L. Effect of water on the properties of epoxy matrix and composite. *Adv Polym Sci* 1985;72:69–77.
- [6] Chateauminos A, Chabert B, Soulier JP, Vincent L. Dynamic-mechanical analysis of epoxy composites plasticized by water – artifact and reality. *Polym Compos* 1995;16(4):288–96.
- [7] Xiao GZ, Shanahan MER. Irreversible effects of hygrothermal aging on DGEBA/DDA epoxy resin. *J Appl Polym Sci* 1998;69(2):363–9.
- [8] Zhou JM, Lucas JP. Hygrothermal effects of epoxy resin. Part I: the nature of water in epoxy. *Polymer* 1999;40(20):5505–12.
- [9] Zhou JM, Lucas JP. Hygrothermal effects of epoxy resin. Part II: variations of glass transition temperature. *Polymer* 1999;40(20):5513–22.
- [10] Xian G, Karbhari VM. DMTA based investigation of hygrothermal ageing of an epoxy system used in rehabilitation. *J Appl Polym Sci* 2007;104(2):1084–94.
- [11] Grave C, McEwan I, Pethrick RA. Influence of stoichiometric ratio on water absorption in epoxy resins. *J Appl Polym Sci* 1998;69(12):2369–76.
- [12] Popineau S, Rondeau-Mouro C, Sulpice-Gaillet C, Shanahan MER. Free/bound water absorption in an epoxy adhesive. *Polymer* 2005;46(24):10733–40.
- [13] Jelinski LW, Dumais JJ, Cholli AL, Ellis TS, Karasz FE. Nature of the water epoxy interaction. *Macromolecules* 1985;18(6):1091–5.
- [14] Woo M, Piggott MR. Water-absorption of resins and composites 1. Epoxy homopolymers and copolymers. *J Compos Technol Res* 1987;9(3):101–7.
- [15] Jelinski LW, Dumais JJ, Stark RE, Ellis TS, Karasz FE. Interaction of epoxy-resins with water – a quadrupole echo deuterium NMR-study. *Macromolecules* 1983;16(6):1019–21.
- [16] Hahn HT. Residual-stresses in polymer matrix composite laminates. *J Compos Mater* 1976;10(Oct):266–78.
- [17] Xiao GZ, Delamar M, Shanahan MER. Irreversible interactions between water and DGEBA/DDA epoxy resin during hydrothermal aging. *J Appl Polym Sci* 1997;65(3):449–58.

- [18] Bao LR, Yee AF. Moisture diffusion and hygrothermal aging in bismaleimide matrix carbon fiber composites — part I: uni-weave composites. *Compos Sci Technol* 2002;62(16):2099–110.
- [19] Grant TS, Bradley WL. In-situ observations in SEM of degradation of graphite-epoxy composite-materials due to seawater immersion. *J Compos Mater* 1995;29(7):852–67.
- [20] Deneve B, Shanahan MER. Water-absorption by an epoxy-resin and its effect on the mechanical-properties and infrared-spectra. *Polymer* 1993;34(24):5099–105.
- [21] Karbhari VM. Dynamic mechanical analysis of the effect of water on E-glass–vinylester composites. *J Reinf Plast Compos* 2006;25(6):631–44.
- [22] Wang JY, Ploehn HJ. Dynamic mechanical analysis of the effect of water on glass bead epoxy composites. *J Appl Polym Sci* 1996;59(2):345–57.
- [23] Akay M, Mun SKA, Stanley A. Influence of moisture on the thermal and mechanical properties of autoclaved and oven-cured Kevlar-49/epoxy laminates. *Compos Sci Technol* 1997;57(5):565–71.
- [24] LaPlante G, Lee-Sullivan P. Moisture effects on FM300 structural film adhesive: stress relaxation, fracture toughness, dynamic mechanical analysis. *J Appl Polym Sci* 2005;95(5):1285–94.
- [25] Kalakkunnath S, Kalika DS, Lin HQ, Freeman BD. Viscoelastic characteristics of UV polymerized poly(ethylene glycol) diacrylate networks with varying extents of crosslinking. *J Polym Sci Part B Polym Phys* 2006;44(15):2058–70.
- [26] Kalakkunnath S, Kalika DS, Lin HQ, Freeman BD. Segmental relaxation characteristics of cross-linked poly(ethylene oxide) copolymer networks. *Macromolecules* 2005;38(23):9679–87.
- [27] Adam G, Gibbs JH. On temperature dependence of cooperative relaxation properties in glass-forming liquids. *J Chem Phys* 1965;43(1):139–47.
- [28] Roland CM, Ngai KL. Segmental relaxation and the correlation of time and temperature dependencies in poly(vinyl methyl-ether) polystyrene mixtures. *Macromolecules* 1992;25(1):363–7.
- [29] Lacik I, Krupa I, Stach M, Kucma A, Jurciova J, Chodak I. Thermal lag and its practical consequence in the dynamic mechanical analysis of polymers. *Polym Test* 2000;19:755–71.
- [30] Hagen R, Salmen L, Lavebratt H, Stenberg B. Comparison of dynamic mechanical measurements and  $T_g$  determination with two different instruments. *Polym Test* 1994;13:113–28.
- [31] Chang TD, Carr SH, Brittain JO. Studies of epoxy-resin systems B. Effect of crosslinking on the physical-properties of an epoxy-resin. *Polym Eng Sci* 1982;22(18):1213–20.
- [32] Bao LR, Yee AF. Effect of temperature on moisture absorption in a bismaleimide resin and its carbon fiber composites. *Polymer* 2002;43(14):3987–97.
- [33] Pascault JP, Sautereau H, Verdu J, Williams RJJ. *Thermosetting polymers*. Marcel Dekker; 2002.
- [34] Ivanova KI, Pethrick RA, Affrossman S. Hygrothermal aging of rubber-modified and mineral-filled dicyandiamide-cured DGEBA epoxy resin. Part II: dynamic mechanical thermal analysis. *J Appl Polym Sci* 2001;82(14):3477–85.
- [35] Ghorbel I, Valentin D. Hydrothermal effects on the physicochemical properties of pure and glass-fiber-reinforced polyester and vinylester resins. *Polym Compos* 1993;14(4):324–34.
- [36] Hough JA, Xiang ZD, Jones FR. The effect of thermal spiking and resultant enhanced moisture absorption on the mechanical and viscoelastic properties of carbon fibre reinforced epoxy laminates. In: *Experimental techniques and design in composite materials 3*, vol. 144; 1998. p. 27–41.
- [37] Ferry JD. *Viscoelastic properties of polymers*. 3rd ed. New York: John Wiley & Sons, Inc.; 1980.
- [38] Williams G, Watts DC. Non-symmetrical dielectric relaxation behaviour arising from a simple empirical decay function. *Trans Faraday Soc* 1970;66:80.
- [39] Goodwin AA, Simon GP. Dynamic mechanical relaxation behaviour of poly(ether ether ketone)/poly(etherimide) blends. *Polymer* 1997;38(10):2363–70.
- [40] Gotze W, Sjogren L. Relaxation processes in supercooled liquids. *Rep Prog Phys* 1992;55(3):241–376.
- [41] Karlsson GE, Gedde UW, Hedenqvist MS. Molecular dynamics simulation of oxygen diffusion in dry and water-containing poly(vinyl alcohol). *Polymer* 2004;45:3893–900.
- [42] Apicella A, Nicolais L, Decataldis C. Characterization of the morphological fine-structure of commercial thermosetting resins through hygrothermal experiments. *Adv Polym Sci* 1985;66:189–207.
- [43] Rizos AK, Ngai KL. Experimental determination of the cooperative length scale of a glass-forming liquid near the glass transition temperature. *Phys Rev E* 1999;59(1):612–7.
- [44] Verghese KNE, Jensen RE, Lesko JJ, Ward TC. Effects of molecular relaxation behavior on sized carbon fiber–vinyl ester matrix composite properties. *Polymer* 2001;42(4):1633–45.
- [45] Bohmer R, Ngai KL, Angell CA, Plazek DJ. Nonexponential relaxations in strong and fragile glass formers. *J Chem Phys* 1993;99(5):4201–9.